



Utility of diffusion tensor imaging in differentiating benign from malignant hepatic focal lesions

Gehad A. Saleh¹ · Ali H. Elmokadem¹ · Ahmed Abdel Razek¹ · Ahmed El-Morsy¹ · Omar Hamdy² · Elshimaa S. Eleraky³ · Marwa Saleh⁴

Received: 9 April 2022 / Revised: 3 August 2022 / Accepted: 5 August 2022 / Published online: 18 August 2022
© The Author(s), under exclusive licence to European Society of Radiology 2022

Abstract

Objectives To assess the diagnostic accuracy of diffusion tensor imaging (DTI) in the characterization of hepatic focal lesions (HFLs) and compare it to diffusion-weighted imaging (DWI).

Methods Prospective analysis was done for 49 patients (23 male and 26 female) with 74 HFLs who underwent dynamic MRI, DWI, and DTI. Apparent diffusion coefficient (ADC) values from DWI, fractional anisotropy (FA) values, and mean diffusivity (MD) values from DTI were measured by two independent radiologists. HFLs were classified into benign and malignant HFLs; the latter were subdivided into HCC and non-HCC lesions. Binary logistic regression was performed to analyze the associations between the DTI parameters and the distinction of malignant lesions.

Results The ADC, MD, and FA at cutoff values of $\leq 1.17 \times 10^{-3} \text{ mm}^2/\text{s}$, $\leq 1.71 \times 10^{-3} \text{ mm}^2/\text{s}$, and > 0.29 , respectively, are excellent discriminators for differentiating malignant and benign HFLs. The mean ADC and MD values of hemangiomas were significantly higher than HCC and non-HCC malignant lesions. In contrast, the mean FA values of hemangiomas were significantly lower than those of non-HCC malignant lesions and HCCs. The ADC and MD were very good discriminators at cutoff values of $> 1.03 \times 10^{-3} \text{ mm}^2/\text{s}$ and $> 1.12 \times 10^{-3} \text{ mm}^2/\text{s}$, respectively. The FA at a cutoff value > 0.38 is an excellent discriminator for HCC versus non-HCC malignant lesions. Only FA value > 0.38 was a statistically significant independent predictor of HCC versus non-HCC lesions among the three parameters. There was an excellent inter-observer agreement with ICC > 0.9 .

Conclusion MD and FA of DTI are non-invasive, very good, and excellent discriminators superior to ADC measured by DWI for the differentiation of HFLs.

Key Points

- The ADC, MD, and FA at cutoff values of $\leq 1.17 \times 10^{-3} \text{ mm}^2/\text{s}$, $\leq 1.71 \times 10^{-3} \text{ mm}^2/\text{s}$, and > 0.29 , respectively, are excellent discriminators for differentiating malignant and benign HFLs.
- The mean ADC and MD values of hemangiomas were significantly higher than those of HCC and non-HCC malignant lesions. In contrast, the mean FA values of hemangiomas were significantly lower than those of non-HCC malignant lesions and HCCs, respectively.
- Multivariate regression analysis revealed that only FA value > 0.38 was a statistically significant independent predictor of HCC vs. non-HCC lesions. A lesion with FA > 0.38 has 34 times higher odds of being HCC rather than non-HCC lesions

Keywords Magnetic resonance imaging · Diffusion · Carcinoma, hepatocellular · Cholangiocarcinoma · Metastasis

Abbreviations

ADC Apparent diffusion coefficient
DTI Diffusion tensor imaging

DWI Diffusion-weighted imaging
FA Fractional anisotropy
HCC Hepatocellular carcinoma

✉ Ali H. Elmokadem
mokadem83@yahoo.com

¹ Department of Radiology, Mansoura University, El Gomhoria St., Mansoura 35516, Egypt

² Department of Surgical Oncology, Mansoura University, Mansoura, Egypt

³ Department of Internal Medicine, Horus University, Damietta, Egypt

⁴ Department of Internal Medicine, Mansoura University, Mansoura, Egypt

HFLs Hepatic focal lesions
MD Mean diffusivity

Introduction

Hepatic tumors constitute a significant health problem; early detection and differentiation are critical for accurate management and patient outcomes. Hepatic focal lesions (HFLs) are classified into benign and malignant lesions. Hemangiomas are the most common benign tumor, while hepatocellular carcinoma (HCC) is the commonest primary hepatic malignancy. Moreover, hepatic metastases are more common than primary hepatic tumors [1, 2].

Current technical improvements in contrast-enhanced ultrasound (CEUS), computed tomography (CT), and magnetic resonance imaging (MRI) have facilitated a more frequent diagnosis of benign and malignant HFLs [3]. CT demonstrated significantly higher sensitivity and specificity for HCC detection than sonography [4]. However, CT has a few limitations, such as radiation exposure and lack of high soft tissue resolution compared to MRI, which may cause indeterminate diagnosis [5]. Contrast-enhanced dynamic MR is a keystone for hepatic lesion characterization [6]. According to the latest Liver Imaging Reporting and Data System (LI-RADS), precise diagnosis of HCC depends on five major features according to the enhancement pattern and size. The diffusion restriction is an ancillary feature favoring malignancy, including HCC and other malignant HFLs [7, 8].

Diffusion-weighted imaging (DWI) is a non-contrast technique that has been progressively used to characterize HFLs [9, 10]. DWI allows qualitative and quantitative analysis through the apparent diffusion coefficient (ADC) map and reflects histopathological tissue features but fails to describe diffusion characteristics in anisotropic environments [10, 11]. Though previous studies have revealed the utility of ADC in the characterization of hepatic focal lesions, the ADC values of benign and malignant liver lesions showed considerable overlaps [12–14].

Diffusion tensor imaging (DTI) is an advanced, recently introduced MR technique developed based on DWI. Unlike the uni-directional or three orthogonal directional DWI, DTI measures the diffusivity of water molecules by using six or more different directions of diffusion-sensitive gradients, visually exposing the microstructural characteristics of biological tissues permitting the evaluation of their anisotropic properties [15, 16]. DTI is considered an emerging technique in extra-cranial applications as it was mainly performed to trace white matter fiber in the nervous system [17–19]. It improves the routine DWI module to illustrate the orientational variability, allowing the assessment of diffusion anisotropy [19]. The calculated DTI parameters are mean diffusivity (MD) and fractional anisotropy (FA), which reflect the size and shape

of the diffusion ellipsoids, respectively [20]. FA shows the fraction of anisotropic diffusion to total diffusion [10].

The data available about the role of DTI in assessing HFLs are few and limited to specific focal lesions [10, 16]; most of the existing data were concerned with the role of DTI in diffuse liver disease as fibrosis and steatosis [15, 21–24]. Furthermore, no available studies compared the diagnostic accuracy of routine DWI and DTI, so we aimed to assess the role of DTI in categorizing HFLs and comparing it to DWI.

Methods

Study population

The institutional review board approved the study, and informed consent was obtained from all patients. Patients with HFLs (> 1 cm) diagnosed by sonography or triphasic CT were included in this study. All patients underwent contrast-enhanced dynamic MRI of the liver, DWI, and DTI from July 2020 to August 2021. Eighteen patients were excluded from the study; 11 had previous locoregional treatment for HCC, 5 had received chemotherapy for hepatic metastases, and the other 2 were due to image quality degradation caused by respiratory motion artifacts. Lastly, 49 patients with 74 focal lesions (23 male and 26 female) were included in the study. Their mean age \pm SD was 51.6 ± 7.1 years, ranging from 30 to 67 years. Figure 1 shows a flow chart of the study population.

MR imaging technique

Conventional MRI

All patients underwent MRI examination at 1.5 T (Ingenia®, Philips Healthcare). Pre-contrast MRI sequences included T1WI (TR/TE = 112/4.8 ms), T2WI (TR/TE \geq 400/80 ms), and T2 SPAIR (spectral adiabatic inversion recovery) fat suppression sequence (TR/TE = 2500–3000/80–100 ms). Gadolinium-based contrast agent (Gd-DTPA) was injected at a dose of 0.1 mmol/kg at a rate of 2 mL/s using an automated injector. Multiphase post-contrast T1-weighted high-resolution isotropic volume examination (THRIVE) was performed, including early and late arterial and portal venous with 18–21-s intervals for image acquisition, and 5-min delayed phases. The following acquisition parameters were used: TR/TE 3.3–4.5/1.4–1.9 ms, flip angle 10°, matrix size 172 \times 135, FOV 300–400 mm, and slice thickness of 3–5 mm.

DWI

DWI was performed before the contrast study using a fat-suppressed single-shot echo-planar sequence with *b* values

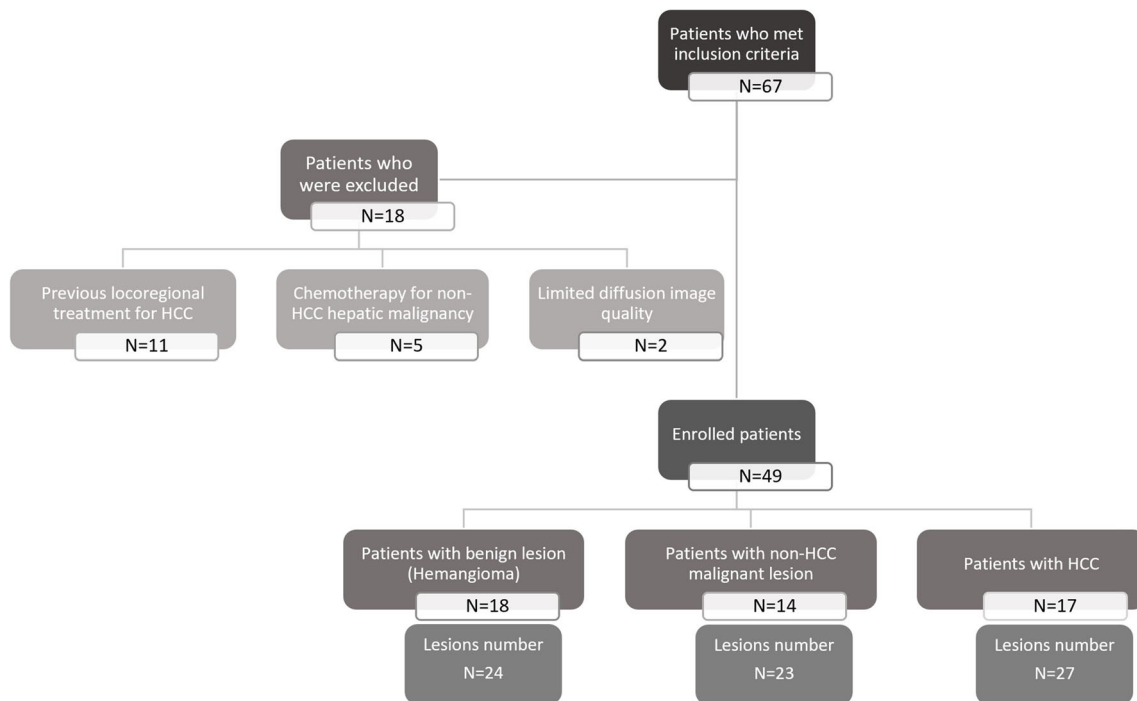


Fig. 1 Flow chart of the study

($b = 0, 500, \text{ and } 1000 \text{ s/mm}^2$). Diffusion imaging acquisition parameters were as follows: TR/TE = 1900–70 ms, NEX = 3, matrix = 124×120 , slice thickness = 5 mm, slice gap = 1–2 mm, and scan time = 70 s.

DTI

Diffusion tensor imaging was also performed before contrast medium injection using axial non-breath hold, single-shot gradient echo-planar DTI sequence (TR/TE = 3000/90 ms). Six diffusion directions were applied along 32 axes using variable diffusion-weighted b values ($b = 0$ and 800 s/mm^2) with the following scanning parameters: FOV = $250 \times 170 \text{ mm}^2$, matrix = 80×60 , and voxel dimensions = $3.5 \times 37 \times 2.5 \text{ mm}^3$. Slice thickness was 2.5 mm with no gap, and total scan duration was 6 min.

Image analysis

Dynamic MR, DWI, and DTI image analysis was performed by two independent radiologists (10 and 5 years of experience in interpreting abdominal MR images). Both radiologists were blinded to the final pathological results in patients with atypical HFLs. The images were transferred to a workstation (extended MR Workspace 2.6.3.5, Philips Medical Systems).

Conventional MRI

Based on the imaging features, HFLs were classified into three groups: benign, HCCs, and non-HCC malignant lesions. We

considered the imaging features of dynamic MRI as the standard of reference for typical HFLs in 41 patients. Atypical HFLs in 8 cases underwent tissue biopsy. Marked T2 hyperintensity and typical enhancement pattern on DCE-MRI (peripheral interrupted nodular enhancement in the arterial phase and progressive centripetal enhancement in the portal and delayed phases) were used to diagnose hemangioma [25]. We used major and ancillary imaging criteria of the latest update of LI-RADS for the diagnosis of HCC as follows: non-rim arterial phase hyperenhancement (APHE) with non-peripheral washout or enhancing capsule in the portal or delayed phases, mild to moderate T2 hyperintensity, and diffusion restriction [7, 8]. HFLs were considered metastatic if a primary tumor was present. Hepatic metastases were diagnosed by the typical appearance of the targetoid mass in the form of rim APHE, peripheral washout, and targetoid diffusion restriction [7, 10]. Intrahepatic mass forming cholangiocarcinoma was diagnosed by minor peripheral rim enhancement during both the arterial and portal venous phases, gradual centripetal prolonged enhancement in the delayed phase with peripheral intrahepatic duct dilatation, and capsular retraction [26].

DWI

Both reviewers measured ADC values separately by manually applying the region of interest (ROI) encompassing the solid part of the HFLs without including the adjacent hepatic parenchyma. The ADC values were measured three times, and the measurements were averaged. In patients with multiple

HFLs, each lesion was determined by its location in the liver (according to the hepatic segment) to avoid overlap between the two observers and then analyzed separately. Moreover, the average ADC value was calculated for each lesion.

DTI

The images were loaded to the DTI software provided by the vendor, and both FA maps and MD maps were created from the post-processing workstation. Co-registration of the MD and FA maps to both T2-weighted and contrast-enhanced T1-weighted images was done for accurate assignment of ROI. A circular ROI was placed on the MD and FA maps over the most enhanced region of the HFL, guided by contrast-enhanced images to avoid cystic or necrotic parts. The ROI size varied from 1 to 3.1 cm² (mean 1.6 cm²). Both observers independently measured MD and FA values three times, and the measurements were averaged. Similarly, in patients with multiple HFLs, both DTI parameters were calculated for each lesion.

Statistical analysis

Data were analyzed using IBM-SPSS software (version 26.0) and MedCalc Statistical Software (version 18.9.1). Quantitative data were initially tested for normality using Shapiro-Wilk's test, with data being normally distributed if $p > 0.050$. The presence of significant outliers was tested by inspecting boxplots. Quantitative data were expressed as mean \pm SD for normally distributed data. The intraclass correlation coefficient (ICC) and Bland and Altman plot were used to assess the agreement between the two raters. One-way ANOVA test compared quantitative data between the three groups. The diagnostic performance of a test was assessed by ROC curve analysis, sensitivity, specificity, PPV, NPV, accuracy, F1 score, and the Matthews Correlation Coefficient. Logistic regression was used to predict the probability that an observation falls into one of two categories of a dichotomous dependent variable (HCC vs. non-HCC). For any of the used tests, results were considered statistically significant if the p value ≤ 0.050 .

Results

Patients' characteristics

Hepatic focal lesions were 24 hemangiomas in 18 patients, 27 HCCs in 17 patients, and 23 non-HCC malignant lesions in 14 patients (9 patients with 18 metastases and 5 patients with cholangiocarcinoma). Six patients with hepatic metastases had primary colorectal cancer, one patient had pancreatic adenocarcinoma, and the last two patients had ovarian cancer.

Out of 14 patients with non-HCC malignancy, eight underwent tissue biopsy (3 with metastases and five cholangiocarcinomas). The remaining six patients were considered metastatic due to known primary malignancy and typical targetoid mass appearance on both dynamic MRI and DWI. No biopsy was performed for benign HFLs or HCCs; the diagnosis was based on MRI features. HCCs were more common in males (85%) than in females (15%). In comparison, hemangiomas were more common in females (75%) than in males (25%). This difference in gender distribution was statistically significant ($p < 0.0005$).

Benign versus malignant HFLs

The ADC, MD, and FA at cutoff values of $\leq 1.17 \times 10^{-3}$ mm²/s, $\leq 1.71 \times 10^{-3}$ mm²/s, and > 0.29 , respectively, were excellent discriminators for differentiating malignant and benign HFLs. This minor difference between the AUC of FA vs. AUCs of both ADC and MD is not statistically significant ($p = 0.2641$). The three parameters have an excellent diagnostic performance with 100% specificity and 100% PPV for all of them (Tables 1 and 2; Fig. 2).

Hemangioma versus HCC and non-HCC malignant lesions

The mean ADC and MD values of hemangiomas ($1.74 \pm 0.18 \times 10^{-3}$ mm²/s and $2.34 \pm 0.21 \times 10^{-3}$ mm²/s, respectively) were significantly higher than those of HCC ($1.07 \pm 0.07 \times 10^{-3}$ mm²/s and $1.22 \pm 0.12 \times 10^{-3}$ mm²/s respectively) and non-HCC malignant lesions ($0.92 \pm 0.11 \times 10^{-3}$ mm²/s and $1.11 \pm 0.10 \times 10^{-3}$ mm²/s respectively) while the mean FA values of hemangiomas (0.25 ± 0.02) were significantly lower than those of non-HCC malignant lesions (0.35 ± 0.05) and HCCs (0.45 ± 0.05). One-way ANOVA test revealed a statistically significant difference in DTI parameters between the three groups, with a large effect size ($f = 2.84, 2.12, \text{ and } 3.67$, for ADC, FA, and MD, respectively). Post hoc tests revealed that the MD values were statistically significantly higher in benign lesions $>$ HCC lesions $>$ non-HCC lesions (Tables 3 and 4).

Table 1 Diagnostic performance of discriminators of malignant vs. benign lesion. Areas under the ROC curves for the three discriminators

Discriminator	Cutoff value	p value	AUC	95% CI	SE
ADC	≤ 1.17	< 0.001	1.000	0.951–1.000	0.0000
FA	> 0.29	< 0.001	0.978	0.913–0.998	0.0197
MD	≤ 1.71	< 0.001	1.000	0.951–1.000	0.0000

Notes: AUC, area under the ROC curve; CI, confidence interval; SE, standard error.

Table 2 Diagnostic performance of discriminators of malignant vs. benign lesion. Diagnostic performance of the three discriminators

Discriminator	SN	SP	PPV	NPV	Accuracy	F1 score	MCC
ADC	100%	100%	100%	100%	1.00	1.00	1.00
FA	96%	100%	100%	92.3%	0.97	0.98	0.94
MD	100%	100%	100%	100%	1.00	1.00	1.00

Notes: *SN*, sensitivity; *SP*, specificity; *PPV*, positive predictive value; *NPV*, negative predictive value; *MCC*, Matthews Correlation Coefficient

HCC versus non-HCC malignant lesions

The ADC and MD at cutoff values of $> 1.03 \times 10^{-3} \text{ mm}^2/\text{s}$ and $> 1.12 \times 10^{-3} \text{ mm}^2/\text{s}$, respectively, were very good discriminators for HCC vs. non-HCC lesions, while FA at a cutoff value > 0.38 was an excellent discriminator for HCC vs. non-HCC lesions. This difference between AUC of FA vs. AUC of MD is statistically significant ($p = 0.036$), while the difference between AUC of ADC vs. AUC of MD is not statistically significant ($p = 0.387$). Table 5 shows very good performance of ADC and MD and an excellent performance of FA in discriminating HCC from non-HCC lesions with 74.1%, 88.9%, and 88.9% sensitivity; 87%, 69.6%, and 91.3% specificity; 87%,

77.4%, and 92.3% PPV; 74.1%, 84.2%, and 87.5% NPV; and 0.80, 0.80, and 0.90 accuracy respectively (Fig. 2).

The binary logistic regression analysis was performed to ascertain the effects of $\text{ADC} > 1.03 \times 10^{-3} \text{ mm}^2/\text{s}$, $\text{FA} > 0.38$, and $\text{MD} > 1.12 \times 10^{-3} \text{ mm}^2/\text{s}$ on the likelihood that the malignant lesion will be HCC vs. non-HCC. On univariate analysis, each of the three parameters was a statistically significant predictor of HCC. So, all these three parameters were entered in a multivariate logistic regression model. The model was statistically significant ($\chi^2(3) = 41.526$, p value < 0.001). The model correctly classified 90% of cases with a sensitivity and a specificity of 88.9% and 91.3%, respectively. Of the three predictor variables, only $\text{FA} > 0.38$ was a statistically

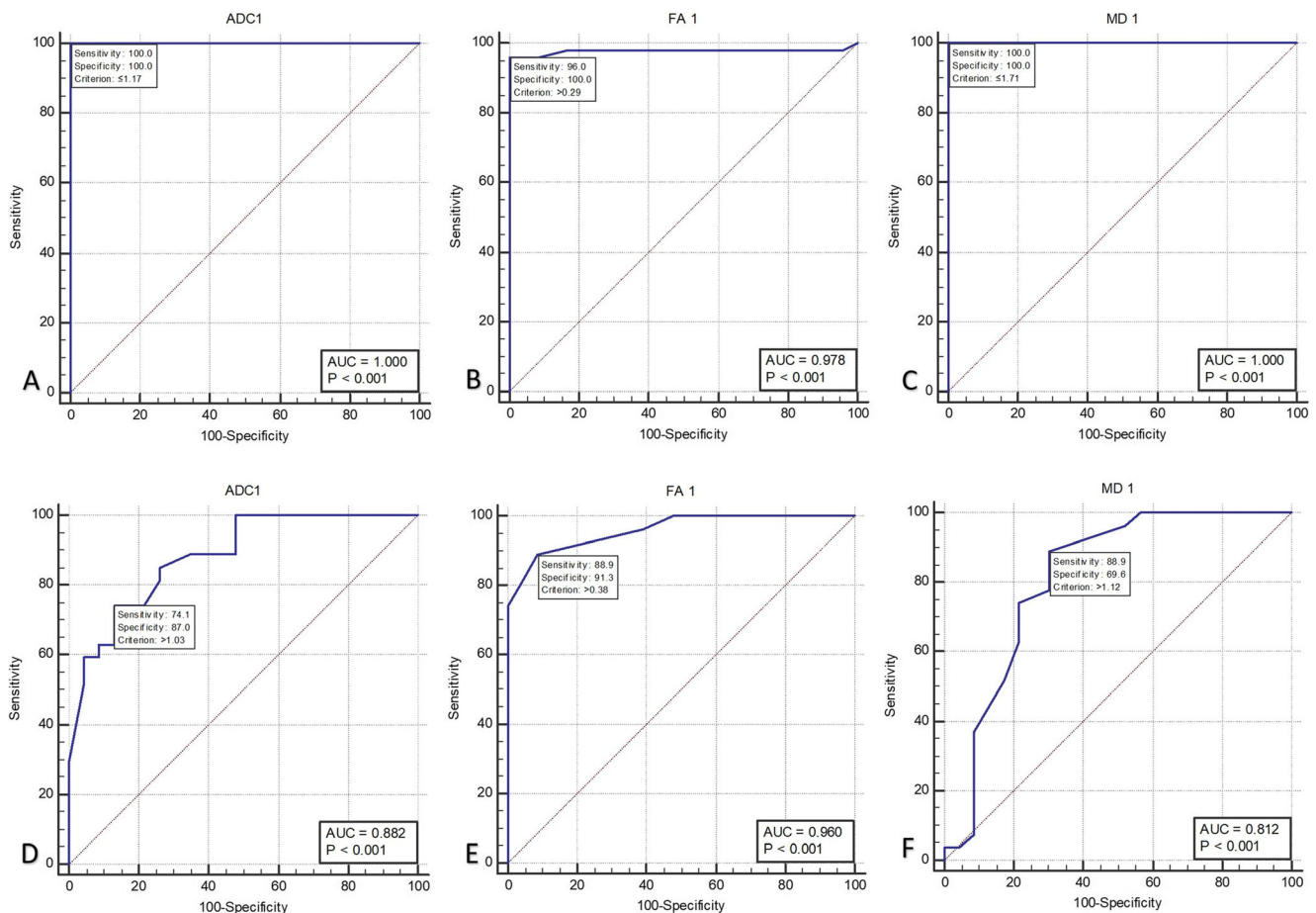


Fig. 2 ROC curves for diagnostic performance of ADC, MD, and FA to discriminate malignant from benign HFLs (A–C). ROC curves for diagnostic performance of ADC, MD, and FA to discriminate HCC from non-HCC malignant lesions (D–F)

Table 3 Diagnostic performance of discriminators of HCC vs. non-HCC. Areas under the ROC curves for the three discriminators

Discriminator	Cutoff value	<i>p</i> value	AUC	95% CI	SE
ADC	> 1.03	< 0.001	0.882	0.760–0.956	0.0458
FA	> 0.38	< 0.001	0.960	0.862–0.995	0.0230
MD	> 1.12	< 0.001	0.812	0.677–0.909	0.0668

Notes: *AUC*, area under the ROC curve; *CI*, confidence interval; *SE*, standard error

significant independent predictor of HCC vs. non-HCC lesions. A lesion with FA > 0.38 has 34 times higher odds of being HCC than non-HCC lesions (Table 6).

Inter-observer agreement

Each observer measured two hundred twenty-two values. There was excellent reliability (absolute agreement) between the two observers in measuring ADC, FA, and MD with ICC = 0.967 and 95% CI = 0.948–0.979, ICC = 0.903 and 95% CI = 0.850–0.937, and ICC = 0.963 and 95% CI = 0.941–0.977 respectively (Fig. 3). Demonstrative cases are listed in Figs. 4, 5, and 6.

Discussion

This study aimed to differentiate between hemangioma, HCC, and non-HCC malignant HFLs, including hepatic metastases

and cholangiocarcinoma, using DWI and DTI parameters. Our results revealed that DTI parameters are excellent discriminators of HFLs as malignant HFLs revealed significantly lower MD and higher FA than benign HFLs. Also, the MD values are statistically significantly higher in hemangiomas > HCC > non-HCC-lesions; only FA > 0.38 was a statistically significant independent predictor of HCC vs. non-HCC-lesions. This study is unique regarding the wide variety of HFLs and the comparison between DWI and DTI.

HCC is the only malignancy for which a non-invasive radiological diagnosis is acceptable based on imaging characteristics on dynamic contrast-enhanced CT or MRI without histological confirmation [27]. Lately, contrast-enhanced CT or MRI has become routinely performed for the diagnosis of HCC and replaced using biopsy to confirm the diagnosis prior to treatment for most patients [28]. The updated LI-RADS system also meets the requirement to accurately diagnose HCC, as it is clinically significant to distinguish between HCC and other hepatic malignancies because the management changes considerably [29]. In this study, we considered LI-RADS-v2018 both major and ancillary imaging features for precisely diagnosing all HCC cases.

Dynamic contrast-enhanced MRI is still the gold standard in HFL characterization. However, contrast media might cause nephropathy in chronic renal insufficiency patients, which is considered the third cause of acute renal injury necessitating hospitalization [30]. This limitation pushed investigators to assess the utility of non-contrast techniques such as DWI in the differentiation between benign and malignant

Table 4 Diagnostic performance of discriminators of HCC vs. non-HCC. Diagnostic performance of the three discriminators

Discriminator	SN	SP	PPV	NPV	Accuracy	F1 score	MCC
ADC	74.1%	87%	87%	74.1%	0.80	0.80	0.61
FA	88.9%	91.3%	92.3%	87.5%	0.90	0.91	0.80
MD	88.9%	69.6%	77.4%	84.2%	0.80	0.83	0.60

Notes: *SN*, sensitivity; *SP*, specificity; *PPV*, positive predictive value; *NPV*, negative predictive value; *MCC*, Matthews Correlation Coefficient

Table 5 Comparison of ADC, FA, and MD between the three study groups

Parameter	Group						One-way ANOVA test (Welsh)		
	Benign		Non-HCC		HCC		<i>F</i> value	<i>p</i> value	Partial η^2
	\bar{x}	SD	\bar{x}	SD	\bar{x}	SD			
ADC	1.74	0.18	0.92	0.11	1.07	0.07	185.38	< 0.001	0.890
FA	0.25	0.02	0.35	0.05	0.45	0.05	208.26	< 0.001	0.818
MD	2.34	0.21	1.11	0.10	1.22	0.12	323.67	< 0.001	0.931

Notes: Data are mean (\bar{x}) and standard deviation (SD). Partial η^2 is a measure of effect size

Table 6 Predictors of the likelihood of HCC vs. non-HCC malignant lesion

Predictor	Univariate			Multivariate		
	COR	95% CI	<i>p</i> value	OR	95% CI	<i>p</i> value
ADC			< 0.001			0.067
≤ 1.03	r (1)	r (1)		r (1)	r (1)	
> 1.03	19	4.3–84.3		6.9	0.88–54.5	
FA			< 0.001			0.002
≤ 0.38	r (1)	r (1)		r (1)	r (1)	
> 0.38	84	12.8–552		33.9	3.6–318	
MD			< 0.001			0.519
≤ 1.12	r (1)	r (1)		r (1)	r (1)	
> 1.12	18.3	4.1–81.4		2.25	0.19–26.6	

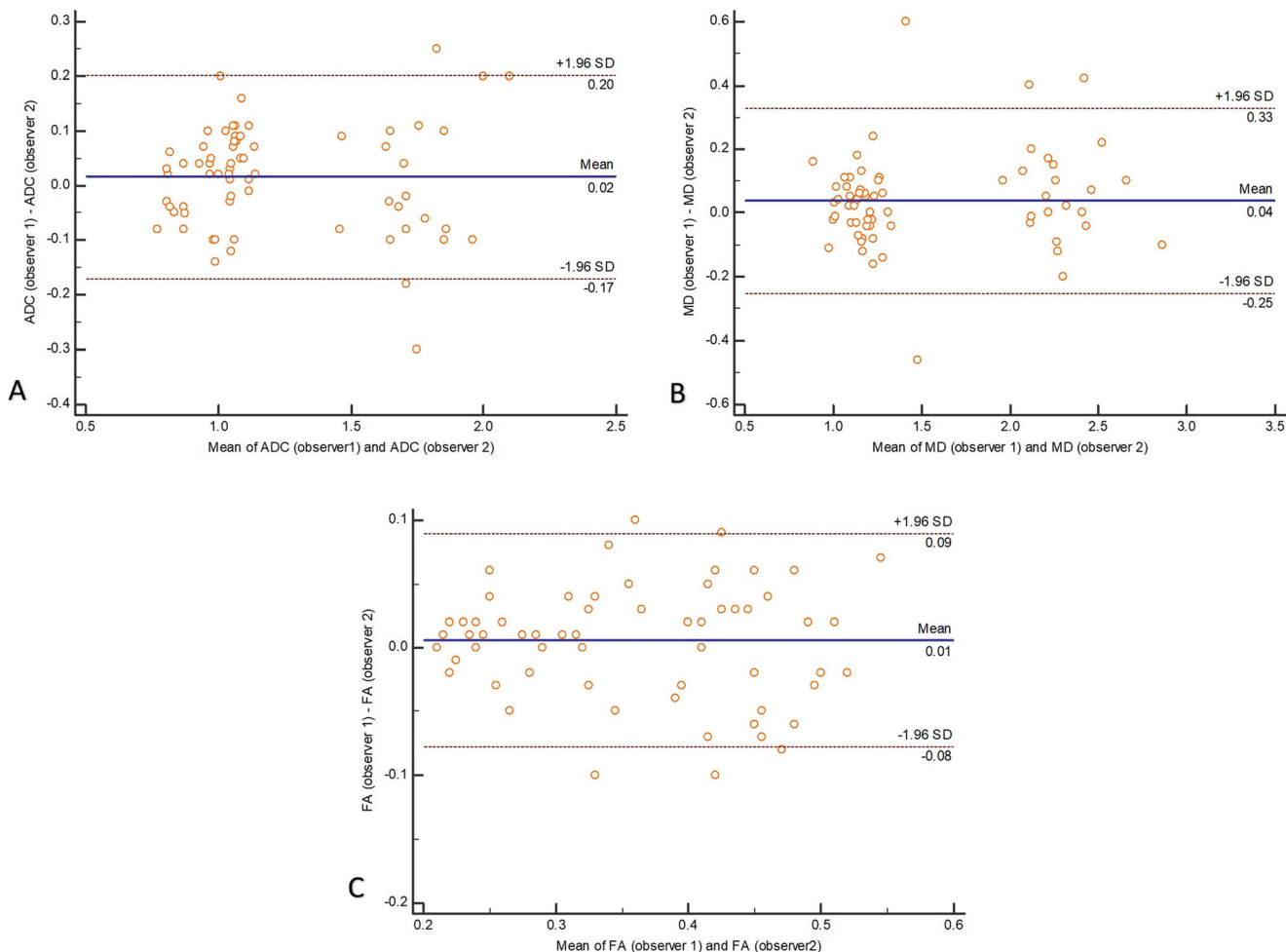
Notes: *r*(1), reference category; *COR*, crude odds ratio; *OR*, odds ratio; *CI*, confidence interval. Test of significance is binary logistic regression

hepatic focal lesions. Prior multiple studies evaluated the value of DWI and measured ADC values in a selected group of HFLs. In concordance with our results, previous studies used

ADC values to differentiate between hemangioma and HCC and stated that ADC values of hemangiomas were significantly higher than those of HCC [31]. Another recent study stated that the combination of quantitative ADC histogram analysis and LI-RADS categorization increases the accuracy of the diagnosis of HCC compared to the other primary liver cancers (ICC and combined HCC-ICC) [32].

On the other hand, there is a substantial overlay between ADC values of benign and malignant lesions. A recent meta-analysis revealed that ADC measurement independently is not an optimal diagnostic imaging method for distinguishing malignant from benign HFLs [33]. Another study added that DWI could not be used as a single criterion of malignant hepatic lesions, as their results revealed a significant difference between benign and malignant HFLs without threshold ADC values for differentiating both categories [34].

Unlike DWI, multiple parameters could be extracted from DTI, including MD and FA. FA values are reported to have a strong correlation with cell density which is considered a good predictor of malignancy [35]. DTI metrics repeatability studies have been performed on the human brain; owing to the

**Fig. 3** Bland-Altman plots for inter-observer reliability of (A) ADC, (B) MD, and (C) FA measurements

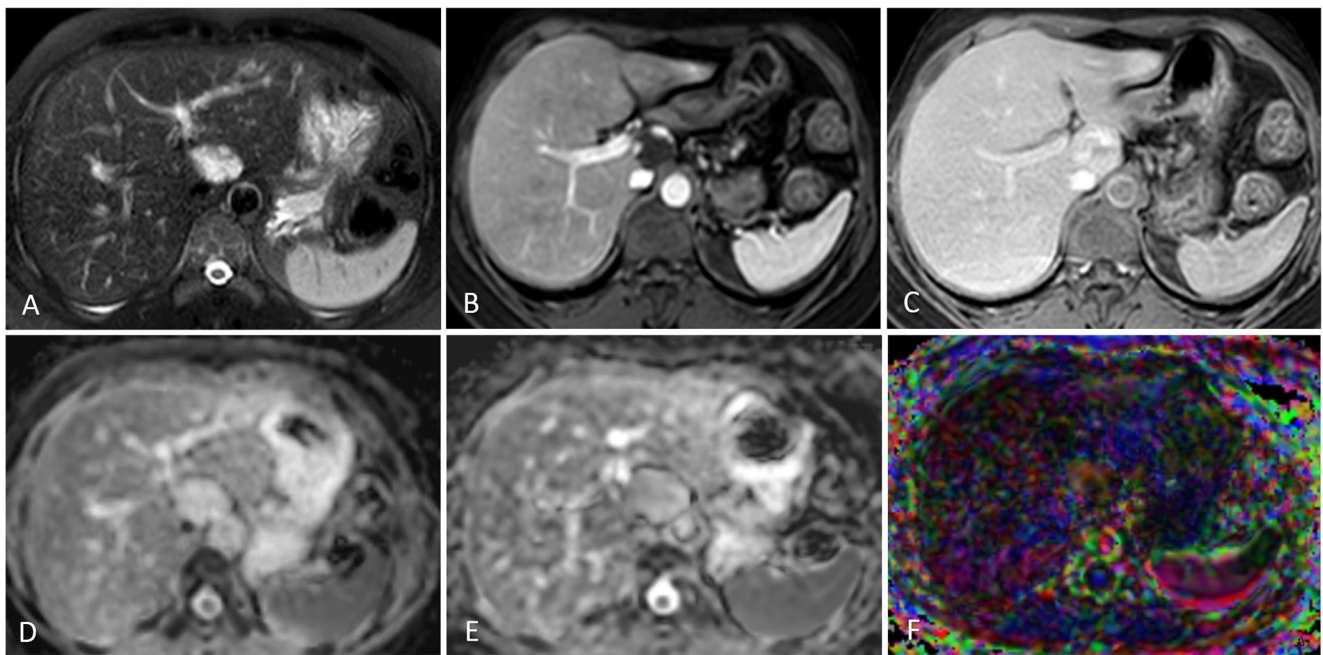


Fig. 4 A 37-year-old female with a segment I hepatic hemangioma: Axial T2 fat-suppressed (A) revealed HFL of bright T2 signal intensity. Axial dynamic arterial and delayed images (B, C) revealed typical peripheral interrupted nodular arterial enhancement with progressive fill-in. Axial

ADC image (D) shows a free diffusion pattern with an ADC value of $1.61 \times 10^{-3} \text{ mm}^2/\text{s}$. In axial MD and colored FA maps (E, F), the hemangioma had an MD value of $2.12 \times 10^{-3} \text{ mm}^2/\text{s}$ and an FA value of 0.26, respectively

anatomical variances between the brain and liver parenchyma, its repeatability in the liver is still under investigation and

needs further confirmation. A recent study revealed that the repeatability of liver DTI metrics improves with an increasing

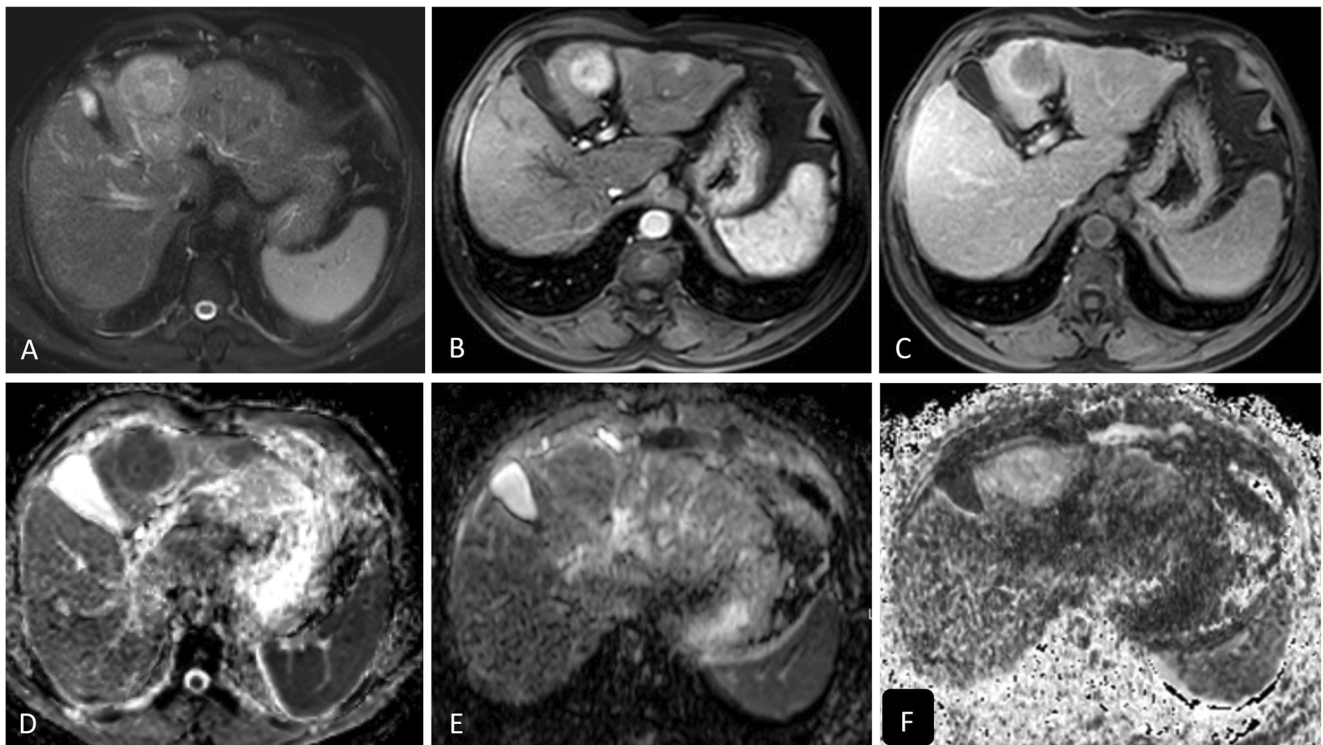
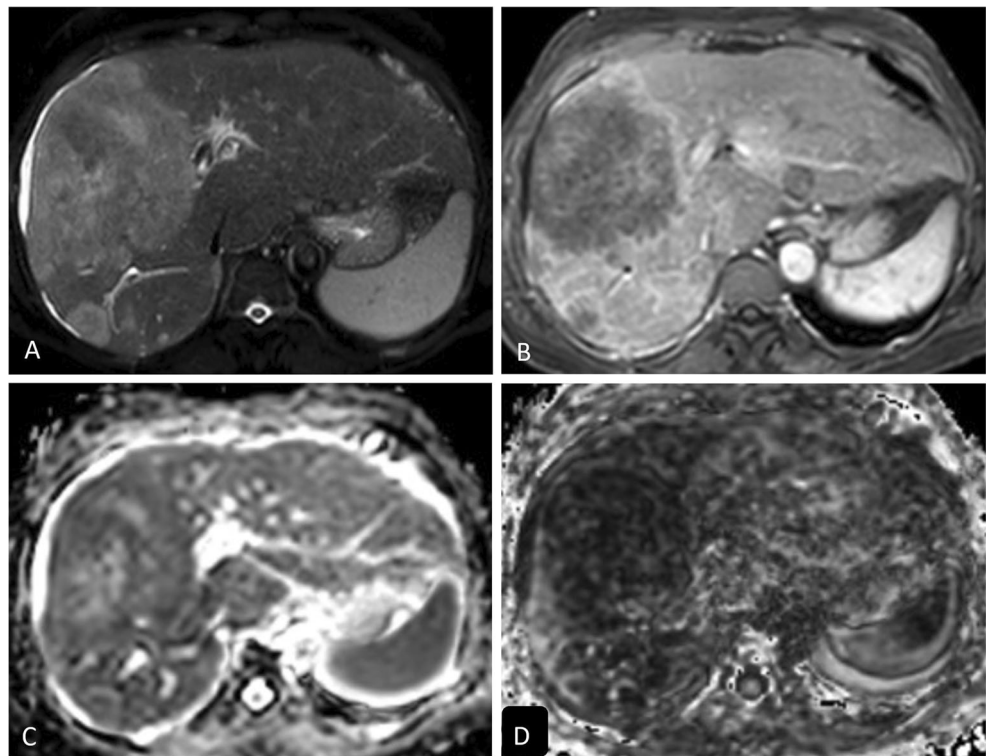


Fig. 5 A 58-year-old male with a segment IV HCC: Axial T2 fat-suppressed image (A) revealed a hepatic focal lesion of intermediate T2 signal intensity. Axial dynamic arterial and delayed images (B, C) revealed typical non-peripheral arterial enhancement with delayed washout.

Axial ADC image (D) shows restricted diffusion with an ADC value of $1.07 \times 10^{-3} \text{ mm}^2/\text{s}$. In axial MD and FA maps (E, F), the HCC had an MD value of $1.21 \times 10^{-3} \text{ mm}^2/\text{s}$ and an FA value of 0.47, respectively

Fig. 6 A 55-year-old male with right lobe cholangiocarcinoma: Axial T2 fat-suppressed image (A) revealed infiltrative lesion at superior segments of the right lobe of high T2 signal intensity with nearby satellite lesions. Axial dynamic arterial image (B) revealed marginal enhancement of the right lobe lesions and left lobe lesions. In axial MD and FA maps (C, D), the cholangiocarcinoma had an MD value of $1.06 \times 10^{-3} \text{ mm}^2/\text{s}$ and an FA value of 0.36, respectively



number of signal averages. However, no benefit was observed with an increasing number of gradient directions beyond six [36].

Few studies have discussed the role of DTI in the assessment of HFLs and were limited to a specific type of lesions [10, 16]. HCC and non-HCC malignant lesions exhibited lower MD than hemangioma, which is assumed to be due to the high cellularity of malignant HFLs as diffusion is impeded by the presence of cellular membranes and macromolecular structures in malignant HFLs. In this study, the FA values of HCC and non-HCC malignant lesions are significantly higher than those of hemangioma, which assumes a higher cell density and malignant character; this is attributed to a moderate/high degree of anisotropy of the malignant HFLs, as the normal structure of cells is often damaged, and consequently, the diffusion directions of water molecules in the tumor are weakened and altered. Furthermore, FA values had a superior performance in discriminating HCC vs. non-HCC malignant lesions compared to MD values. Li et al investigated the feasibility of DTI in the differentiation between HCC and healthy liver without comparing the DTI parameters to routine DWI. They stated that HCC had significantly lower ADC values and higher FA than the healthy liver ($1.30 \pm 0.34 \times 10^{-3} \text{ mm}^2/\text{s}$ vs. $1.52 \pm 0.27 \times 10^{-3} \text{ mm}^2/\text{s}$, $p = 0.013$; and 0.42 ± 0.11 vs. 0.32 ± 0.10 , $p = 0.004$ respectively). Additionally, the DTI cutoff values for HCCs were close to our results [16].

A retrospective study assessed the utility of DTI in the diagnosis of hepatic cysts, hemangioma, and metastases without comparison with DWI [10] and revealed that the mean

ADC value of cysts ($3.30 \pm 0.8 \times 10^{-3} \text{ mm}^2/\text{s}$) was significantly higher than that of hemangiomas ($2.23 \pm 0.5 \times 10^{-3} \text{ mm}^2/\text{s}$) and metastases ($1.62 \pm 0.4 \times 10^{-3} \text{ mm}^2/\text{s}$), while the mean FA value of cysts (0.2 ± 0.05) was significantly lower than of hemangiomas (0.37 ± 0.1) and metastases (0.46 ± 0.1). While metastases tend to have low ADC and high FA values, cysts have high ADC and low FA values, and hemangiomas have high ADC and high FA values. Their result was in concordance with ours. They also concluded that FA values might play a supportive role in the imaging of HFLs. Our study revealed relatively lower MD and FA values for liver metastases which may be attributed to their choice of placing large ROIs, including the cystic parts of the metastases in the measurement, which may have caused an increase in the measured values.

Intrahepatic cholangiocarcinoma (ICC) is the second most common primary liver tumor. The operative management is the gold standard, but ICC is frequently unresectable at diagnosis [37]. Recent studies revealed that the mean ADC of ICC was significantly lower than that of adjacent liver parenchyma; additionally, ADC quantification was helpful for expecting ICC tumor grade [38]. ICC tumors are supplied by the hepatic artery and are classically less vascular than HCCs, thus may be responsible for the lower ADC, MD, and FA values of ICC than HCCs in our study. However, the included ICC cases were few, and further studies are required for a better assessment of the DTI metrics in ICC.

DTI parameters and especially FA values allow better discrimination of HCCs from other non-HCC lesions, which is

critical as they have different management and prognosis. Detection of HCC at early stages permits the application of curative treatments such as ablation, resection, or a transplant improving the patient's prognosis [5]. The addition of FA to MD measurement increased confidence of discriminating HCC from non-HCC malignant lesions as multivariate regression analysis revealed that only FA value > 0.38 was a statistically significant independent predictor of HCC versus non-HCC lesions. A lesion with FA > 0.38 has 34 times higher odds of being HCC than non-HCC lesions.

Contrary to our results, one old study by Taouli et al showed an isotropic diffusion in both benign and malignant HFLs with minor non-significant differences between the ADC values [39]. The MD values of DTI in this study were relatively higher than ADC values of DWI for both benign and malignant HFLs; this may be attributed to 32 diffusion gradients applied in DTI in contrast with three gradients only applied in DWI. To the best of our knowledge, there is no available inter-observer agreement prospective study for discriminating variable HFLs using both DWI and DTI parameters. Our study showed an excellent inter-observer agreement between the two observers in measuring ADC, FA, and MD. A previous retrospective study that investigated the DTI measurements of only 3 types of HFLs (cyst, hemangioma, and metastases) without including DWI revealed very good inter-observer agreement [10].

This study has a few limitations. Firstly, the patient population is a relatively small number. Further multi-center studies upon a larger number of patients are recommended for better data collection. Secondly, the inclusion criteria in this study were patients with HFLs without previous chemotherapy or locoregional treatment. Further studies are recommended to assess DTI accuracy in predicting the response in patients with treated HFLs. Thirdly, this study used two-dimensional ROI to estimate the FA and the MD metrics. The use of three-dimensional ROI for evaluating the entire lesion/volume or advanced post-processing such as diffusion kurtosis and intravoxel incoherent motion (IVIM) diffusion-weighted MR imaging and machine learning [40] might enhance the assessment of HFLs. Several studies evaluated the IVIM technique for assessing liver tumors; nevertheless, they show an overlap of IVIM parameters between liver parenchyma and various pathologies [41]. Lastly, we excluded lesions less than 1 cm from the analysis, and usually, these lesions are difficult to diagnose. Our target was to get accurate cutoff values to differentiate between HFLs without reading bias from nearby healthy parenchyma.

Conclusion

MD and FA of diffusion tensor imaging are non-invasive, reliable, and reproducible excellent discriminators superior

to ADC measured by routine DWI for differentiation of benign hepatic focal lesions as hemangioma from HCC and non-HCC malignant lesions. The FA value for DTI is a statistically significant independent predictor of HCC vs. non-HCC lesions.

Funding The authors state that this work has not received any funding.

Declarations

Guarantor The scientific guarantor of this publication is Ali Elmokadem.

Conflict of interest The authors of this manuscript declare no relationships with any companies whose products or services may be related to the subject matter of the article.

Statistics and biometry One of the authors has significant statistical expertise.

Informed consent Written informed consent was waived by the Institutional Review Board.

Ethical approval Institutional Review Board approval was obtained.

Methodology

- prospective
- diagnostic or prognostic study
- performed at one institution

References

1. Razek AAKA, El-Serougy LG, Saleh GA, Shabana W, Abd El-Wahab R (2020) Reproducibility of LI-RADS treatment response algorithm for hepatocellular carcinoma after locoregional therapy. *Diagn Interv Imaging* 101(9):547–553. <https://doi.org/10.1016/j.diii.2020.03.008>
2. Zaitoun MMA, Elsayed SB, Zaitoun NA et al (2021) Combined therapy with conventional trans-arterial chemoembolization (cTACE) and microwave ablation (MWA) for hepatocellular carcinoma >3 - <5 cm. *Int J Hyperth* 38(1):248–256. <https://doi.org/10.1080/02656736.2021.1887941>
3. Pandey P, Lewis H, Pandey A et al (2017) Updates in hepatic oncology imaging. *Surg Oncol* 26(2):195–206. <https://doi.org/10.1016/j.suronc.2017.03.007>
4. Yoon JH, Lee JM, Lee DH et al (2020) A comparison of biannual two-phase low-dose liver CT and US for HCC surveillance in a group at high risk of HCC development. *Liver Cancer* 9(5):503–517. Available from: <https://www.karger.com/DOI/10.1159/000506834>. <https://doi.org/10.1159/000506834>
5. An JY, Peña MA, Cunha GM et al (2020) Abbreviated MRI for hepatocellular carcinoma screening and surveillance. *Radiographics* 40(7):1916–1931. <https://doi.org/10.1148/rg.2020200104>

6. Donato H, França M, Candelária I, Caseiro-Alves F (2017) Liver MRI: From basic protocol to advanced techniques. *Eur J Radiol* 93:30–39. <https://doi.org/10.1016/j.ejrad.2017.05.028>
7. Razek AAKA, El-Serougy LG, Saleh GA, Shabana W, Abd El-wahab R (2020) Liver imaging reporting and data system version 2018: what radiologists need to know. *J Comput Assist Tomogr* 44(2):168–177. <https://doi.org/10.1097/RCT.0000000000000995>
8. Razek AAKA, El-Serougy LG, Saleh GA, Abd el-wahab R, Shabana W (2020) Interobserver agreement of magnetic resonance imaging of Liver Imaging Reporting and Data System version 2018. *J Comput Assist Tomogr* 44(1):118–123. <https://doi.org/10.1097/RCT.0000000000000945>
9. Taron J, Johannink J, Bitzer M, Nikolaou K, Notohamiprodjo M, Hoffmann R (2018) Added value of diffusion-weighted imaging in hepatic tumors and its impact on patient management. *Cancer Imaging* 18(1):1–7
10. Erturk SM, Ichikawa T, Kaya E et al (2014) Diffusion tensor imaging of cysts, hemangiomas, and metastases of the liver. *Acta Radiol* 55(6):654–660. <https://doi.org/10.1177/0284185113504916>
11. Saleh GA, Alghandour R, Rashad EY, Tawfik AM, Elmokadem AH (2021) The adjunctive value of diffusion weighted imaging in diagnosis and follow up of uterovaginal diffuse B-cell lymphoma: a case report and literature review. *Curr Med Imaging* 17(9):1159–1166
12. Kim HC, Seo N, Chung YE, Park M-S, Choi J-Y, Kim M-J (2019) Characterization of focal liver lesions using the stretched exponential model: comparison with monoexponential and biexponential diffusion-weighted magnetic resonance imaging. *Eur Radiol* 29(9):5111–5120. <https://doi.org/10.1007/s00330-019-06048-4>
13. Parikh T, Drew SJ, Lee VS et al (2008) Focal liver lesion detection and characterization with diffusion-weighted MR imaging: comparison with standard breath-hold T2-weighted imaging. *Radiology* 246(3):812–822. <https://doi.org/10.1148/radiol.2463070432>
14. Taouli B, Koh D-M (2010) Diffusion-weighted MR imaging of the liver. *Radiology* 254(1):47–66. <https://doi.org/10.1148/radiol.09090021>
15. Huang M, Lu X, Wang X, Shu J (2020) Diffusion tensor imaging quantifying the severity of chronic hepatitis in rats. *BMC Med Imaging* 20(1):1–7
16. Li X, Liang Q, Zhuang L et al (2015) Preliminary study of MR diffusion tensor imaging of the liver for the diagnosis of hepatocellular carcinoma. *PLoS One* 10(8):e0135568. <https://doi.org/10.1371/journal.pone.0135568>
17. Razek AAKA, Abdalla A, Elfar R, Ashmalla GA, Ali K, Barakat T (2020) Assessment of diffusion tensor imaging parameters of hepatic parenchyma for differentiation of biliary atresia from Alagille syndrome. *Korean J Radiol* 21(12):1372
18. El-Serougy L, Abdel Razek AAK, Ezzat A, Eldawoody H, El-Morsy A (2016) Assessment of diffusion tensor imaging metrics in differentiating low-grade from high-grade gliomas. *Neuroradiol J* 29(5):400–407. <https://doi.org/10.1177/1971400916665382>
19. Razek AAKA (2018) Routine and advanced diffusion imaging modules of the salivary glands. *Neuroimaging Clin* 28(2):245–254
20. Koontz NA, Wiggins RH III (2017) Differentiation of benign and malignant head and neck lesions with diffusion tensor imaging and DWI. *AJR Am J Roentgenol* 208(5):1110–1115. <https://doi.org/10.2214/AJR.16.16486>
21. Tosun M, Inan N, Sarisoy HT et al (2013) Diagnostic performance of conventional diffusion weighted imaging and diffusion tensor imaging for the liver fibrosis and inflammation. *Eur J Radiol* 82(2):203–207. <https://doi.org/10.1016/j.ejrad.2012.09.009>
22. Taouli B, Chouli M, Martin AJ, Qayyum A, Coakley FV, Vilgrain V (2008) Chronic hepatitis: role of diffusion-weighted imaging and diffusion tensor imaging for the diagnosis of liver fibrosis and inflammation. *J Magn Reson Imaging An Off J Int Soc Magn Reson Med* 28(1):89–95
23. Lee Y, Kim H (2015) Assessment of diffusion tensor MR imaging (DTI) in liver fibrosis with minimal confounding effect of hepatic steatosis. *Magn Reson Med* 73(4):1602–1608. <https://doi.org/10.1002/mrm.25253>
24. Cheung JS, Fan SJ, Gao DS, Chow AM, Man K, Wu EX (2010) Diffusion tensor imaging of liver fibrosis in an experimental model. *J Magn Reson Imaging* 32(5):1141–1148. <https://doi.org/10.1002/jmri.22367>
25. Tamada T, Ito K, Yamamoto A et al (2011) Hepatic hemangiomas: evaluation of enhancement patterns at dynamic MRI with gadoxetate disodium. *AJR Am J Roentgenol* 196:824–830
26. Chung YE, Kim MJ, Park YN et al (2009) Varying appearances of cholangiocarcinoma: radiologic pathologic correlation. *Radiographics* 29:683–700. <https://doi.org/10.1148/rg.293085729>
27. Bota S, Piscaglia F, Marinelli S, Pecorelli A, Terzi E, Bolondi L (2012) Comparison of international guidelines for non-invasive diagnosis of hepatocellular carcinoma. *Liver Cancer* 1(3–4):190–200
28. Harris PS, Hansen RM, Gray ME et al (2019) Hepatocellular carcinoma surveillance: an evidence-based approach. *World J Gastroenterol* 25:1550–1559. <https://doi.org/10.3748/wjg.v25.i13.1550>
29. Saleh G, Razek AKA, El-Serougy L, Shabana W, El-Wahab R (2022) The value of the apparent diffusion coefficient value in the Liver Imaging Reporting and Data System version 2018. *Pol J Radiol* 87(1):43–50. <https://doi.org/10.5114/pjr.2022.113193>
30. Ledneva E, Karie S, Launay-Vacher V, Janus N, Deray G (2009) Renal safety of gadolinium-based contrast media in patients with chronic renal insufficiency. *Radiology* 250(3):618–628. <https://doi.org/10.1148/radiol.2503080253>
31. Nam SJ, Yu J-S, Cho E-S, Kim JH, Chung J-J (2017) High-flow haemangiomas versus hypervascular hepatocellular carcinoma showing “pseudo-washout” on gadoxetic acid-enhanced hepatic MRI: value of diffusion-weighted imaging in the differential diagnosis of small lesions. *Clin Radiol* 72(3):247–254. <https://doi.org/10.1016/j.crad.2016.09.020>
32. Lewis S, Peti S, Hectors SJ et al (2019) Volumetric quantitative histogram analysis using diffusion-weighted magnetic resonance imaging to differentiate HCC from other primary liver cancers. *Abdom Radiol (NY)* 44(3):912–922. <https://doi.org/10.1007/s00261-019-01906-7>
33. Nalaini F, Shahbazi F, Mousavinezhad SM, Ansari A, Salehi M (2021) Diagnostic accuracy of apparent diffusion coefficient (ADC) value in differentiating malignant from benign solid liver lesions: a systematic review and meta-analysis. *Br J Radiol* 94:20210059. <https://doi.org/10.1259/bjr.20210059>
34. Oussous SA, Boujraf S, Kamaoui I (2016) Assessment of the focal hepatic lesions using diffusion tensor magnetic resonance imaging. *J Med Signals Sens* 6(2):99
35. Kinoshita M, Hashimoto N, Goto T et al (2008) Fractional anisotropy and tumor cell density of the tumor core show positive correlation in diffusion tensor magnetic resonance imaging of malignant brain tumors. *Neuroimage* 2008 43(1):29–35
36. Wong OL, Leung TWT, Lo GG, Yuan J, Li WW, Noseworthy MD (2017) Intrasession and intersession repeatability of diffusion tensor imaging in healthy human liver. *J Comput Assist Tomogr* 41(4):578–585. <https://doi.org/10.1097/RCT.0000000000000572>
37. Gupta A, Dixon E (2017) Epidemiology and risk factors: intrahepatic cholangiocarcinoma. *Hepatobiliary Surg Nutr* 6(2):101. <https://doi.org/10.21037/hbsn.2017.01.02>
38. Lewis S, Besa C, Wagner M et al (2018) Prediction of the histopathologic findings of intrahepatic cholangiocarcinoma: qualitative and quantitative assessment of diffusion-weighted imaging. *Eur Radiol* 28(5):2047–2057. Available from: <https://doi.org/10.1007/s00330-017-5156-6>

39. Taouli B, Vilgrain V, Dumont E, Daire J-L, Fan B, Menu Y (2003) Evaluation of liver diffusion isotropy and characterization of focal hepatic lesions with two single-shot echo-planar MR imaging sequences: prospective study in 66 patients. *Radiology* 226(1):71–78. <https://doi.org/10.1148/radiol.2261011904>
40. Alksas A, Shehata M, Saleh GA et al (2021) A novel computer-aided diagnostic system for accurate detection and grading of liver tumors. *Sci Rep* 11(1):1–18
41. Li YT, Cercueil JP, Yuan J, Chen W, Loffroy R, Wang YX (2017) Liver intravoxel incoherent motion (IVIM) magnetic resonance imaging: a comprehensive review of published data on normal values

and applications for fibrosis and tumor evaluation. *Quant Imaging Med Surg* 7(1):59–78. <https://doi.org/10.21037/qims.2017.02.03>

Publisher's note Springer Nature remains neutral with regard to jurisdictional claims in published maps and institutional affiliations.

Springer Nature or its licensor holds exclusive rights to this article under a publishing agreement with the author(s) or other rightsholder(s); author self-archiving of the accepted manuscript version of this article is solely governed by the terms of such publishing agreement and applicable law.